Journal of Fusion Energy (2019) 38:315–329
https://doi.org/10.1007/s10894-018-0182-1

ORIGINAL RESEARCH

Fusion Neutrons: Tritium Breeding and Impact on Wall Materials and Components of Diagnostic Systems

Marek Rubel[1]

Published online: 1 September 2018

Abstract
A concise overview is given on the impact of fusion neutrons on various classes of materials applied in reactor technology: plasma-facing, structural and functional tested for tritium production and for diagnostic systems. Tritium breeding in the reactor blanket, fuel cycle and separation of hydrogen isotopes are described together with issues related to primary (tritium) and induced radioactivity. Neutron-induced damage and degradation of material properties are addressed. Material testing under neutron fluxes and safety issues associated with handling components in the radioactive environment are described. A comprehensive list of references to monographs and research papers is included to help navigation in literature.

Keywords Controlled fusion · Tritium · Radiation damage · Transmutation · Fuel cycle

Introduction

The driving force and the main goal of research on controlled thermonuclear fusion is to construct a power generating system based on the energy output of nuclear reactions between light isotopes. Processes under consideration involve deuterium (symbol D, d or ^{2}H), tritium (T, t or ^{3}H) and ^{3}He:

$$\mathrm{D} + \mathrm{T} \rightarrow \alpha(3.52\ \mathrm{MeV}) + \mathrm{n}(14.06\ \mathrm{MeV}) \quad (1)$$

$$\mathrm{D} + {}^{3}\mathrm{He} \rightarrow \alpha(3.67\ \mathrm{MeV}) + \mathrm{H}(14.69\ \mathrm{MeV}) \quad (2)$$

$$\mathrm{D} + \mathrm{D} \rightarrow \mathrm{T}(1.01\ \mathrm{MeV}) + \mathrm{H}(3.03\ \mathrm{MeV}) \quad (3a)$$

$$\mathrm{D} + \mathrm{D} \rightarrow {}^{3}\mathrm{He}(0.82\,\mathrm{MeV}) + \mathrm{n}(2.45\,\mathrm{MeV}) \quad (3b)$$

$$\mathrm{T} + \mathrm{T} \rightarrow {}^{4}\mathrm{He}(3.77\,\mathrm{MeV}) + 2\mathrm{n}(7.53\,\mathrm{MeV}) \quad (4)$$

The branching ratio of Reactions (3a) and (3b) is around one.

The energy release (Q value) and cross-sections (σ) of respective nuclear reactions indicate that the deuterium–tritium fusion, Reaction (1), is the best possible option [1, 2]. The reaction's cross-section (σ) is greater than that of other processes listed above. The maximum is around 70 keV (700,000,000 K) of deuteron energy but high D–T reactivity is reached already at 20 keV. Cross-section values of other processes are significantly lower and their maxima are above hundreds of keV, what—in other words—would require efficient particle heating and their confinement at the temperature of 2×10^{9} K or even higher. As a consequence, at present, all plans and efforts towards commercial fusion are concentrated on a reactor fuelled with deuterium and tritium. Two main schemes of fusing nuclei are: (1) magnetic confinement fusion (MCF) of plasma ignited and maintained by strong magnetic field of several tesla [3] and (2) inertial confinement (ICF) by intense laser [4] or ion beams [5]. Many scientific and technological issues and challenges are similar in all these approaches, especially when it comes to production of tritium fuel. In the following only the first scheme will be discussed, because it is most matured from the reactor technology point of view.

In every method of energy production, from hydro, via fossil materials, windmills to nuclear, the most important and indispensable factor is the fuel and its availability. Experiments in present-day controlled fusion devices are carried out mostly with easily available deuterium (Reactions 3a, 3b), but in the past experimental campaigns with

✉ Marek Rubel
rubel@kth.se

[1] Royal Institute of Technology (KTH), 100 44 Stockholm, Sweden

D–T mixture (including 1:1 D–T operation) were performed at the Joint European Torus (JET) [6–8] and Tokamak Fusion Test Reactor (TFTR) [9]. The next D–T campaign in JET at the Culham Science Centre, UK is planned in year 2019. A step forward is expected to be done in the International Thermonuclear Experimental Reactor (ITER) constructed by seven partners to demonstrate high power performance operation and generation of tritium.

The aim of this lecture is to give an introduction to issues related to fusion neutrons which are energy carriers. They are indispensable for tritium breeding, but they also modify properties of wall materials causing radiation damage and transmutation. First the D–T reaction and its consequences are described. Then tritium breeding and fuel cycle are introduced and it is followed by the description of requirements for plasma-facing and reactor materials. Transmutation and radiation damage are presented in the next paragraph in which also the impact of neutrons on material performance is addressed. The work is concluded with remarks material testing and on safety issues associated with handling components in radioactive environment.

Deuterium–Tritium Fusion Reaction: Reactants and Consequences

In this paragraph all components of the D–T reaction are discussed because each of them plays an important and unique role. Deuterium and tritium are fuel species. The Q value of their reaction is 17.58 MeV of which, according to kinematics, 3.52 MeV is associated with fast alpha particle and 14.06 MeV is carried away by a fast neutron. A complete burn of 1 g of the equimolar D–T mixture corresponds to 1.2×10^{23} reactions producing energy of 67.9 GJ and 271.8 GJ carried by alphas and neutrons, respectively. Alpha particles are to transfer their energy to plasma thus enabling its efficient heating to achieve self-sustaining fusion. However, it also means that eventually the radiated power transferred from alphas to the fuel must be extracted by plasma-facing materials (PFM) and components (PFC). Fast neutrons are to deposit their energy in the absorber (reactor blanket) to facilitate heat exchange and transfer to electricity generating systems of a power plant and, simultaneously, for tritium production via nuclear reactions in the blanket.

The best way to exemplify the general power balance into consider a reactor of, for instance, 500 MW of fusion power. 80% of that (i.e. 400 MW) will be associated with neutrons and the rest (100 MW) with alphas. To the latter number one must add power injected by auxiliary heating systems, approximately 50 MW (neutral beam injection and resonance methods), is to be radiated by plasma and removed by PFC, i.e. 150 MW in total.

In summary, the reaction provides all necessary information regarding the direction how to proceed towards the main goal. However, it also indicates and signalises serious consequences and technological challenges related to power exhaust and radioactivity connected with the use of tritium and neutron-induced activation of plasma-surrounding structures. Neutrons are energy carriers, but—when passing through the surrounding wall components—they cause serious modification of structural (walls) and functional (diagnostics) materials. It is stressed here that issues related to power handling and exhaust, radiation damage and tritium breeding are universal for all confinement schemes realised for energy generation.

Tritium Breeding and Tritium Plant

Tritium is a low-energy β^- emitter:

$$\mathrm{T}(\beta^-) \rightarrow {}^3\mathrm{He}\,(18.59\,\mathrm{keV},\ t_{1/2} = 12.323\,\mathrm{years}). \quad (5)$$

Resulting radioactivity of 1 g T equals to 9652 Ci (3.571×10^{14} Bq). In nature it is formed by the interaction of cosmic rays with atmospheric gases. The first step is the generation of neutrons which then interact with nitrogen:

$${}^{14}\mathrm{N} + \mathrm{n} \rightarrow {}^{12}\mathrm{C} + \mathrm{T} - 4.3\,\mathrm{MeV} \quad (6)$$

$${}^{14}\mathrm{N} + \mathrm{n} \rightarrow 3\,{}^4\mathrm{He} + \mathrm{T} - 11.5\,\mathrm{MeV}. \quad (7)$$

These processes yield annually around 150 PBq of tritium (1.5×10^{17} Bq, approximately 0.411 kg). The total inventory resulting from the global equilibrium (formation and decay) amounts to 2590 PBq ($\sim$ 7.2 kg). A small amount of tritium is also formed by the reaction of neutrons in rocks containing lithium (the main reaction is with ^{6}Li), boron, uranium and thorium [10]. In summary, tritium does not occur in nature in quantities to be considered as resources sufficient for reactor operation. According to the estimates one requires around 168 kg tritium per year for a reactor of 3 GW_{th} [2].

Tritium Breeding

The data shown above clearly indicate that tritium for a D–T reactor is to be produced specially for that purpose. It should be stressed that there are no tritium factories (and no such plans) to generate required huge amounts of tritium to supply a fusion plant. Tritium for many applications, including military, is generated nowadays in nuclear reactors as a minor fission product of ^{235}U, ^{233}U and ^{239}Pu (1 atom generated in 10^4 acts of fission) and in reactions of neutrons with deuterium (in heavy water nuclear reactors),

lithium-6 or boron-10. Availability and production rates of T in CANDU reactors are discussed in [11]: around 100 g per reactor per year. Therefore, tritium for a fusion reactor must be produced on site, directly in the reactor blanket. Breeding based on reactions of neutrons with lithium is the choice. The element has two stable isotopes ^{6}Li and ^{7}Li with natural abundance of 7.59% and 92.41%, respectively. They are transmuted to tritium in following reactions:

$$^{6}\mathrm{Li} + \mathrm{n} \rightarrow \alpha + \mathrm{T} + 4.78\,\mathrm{MeV} \quad (E_{th} = 2.47\,\mathrm{MeV}), \tag{8}$$

$$^{7}\mathrm{Li} + \mathrm{n} \rightarrow \alpha + \mathrm{T} + \mathrm{n}' - 2.47\,\mathrm{MeV}, \tag{9}$$

$$^{7}\mathrm{Li} + \mathrm{n} \rightarrow 2\mathrm{T} + 2\mathrm{n}' - 10.3\,\mathrm{MeV}, \tag{10}$$

where E_{th} denotes the threshold energy of the process. All three reactions yield neutrons but physics of processes clearly indicates benefits of using ^{6}Li. The reaction cross-section increases with the decreasing neutron energy and, as obtained using JENDL-4.0 (Japanese Evaluated Nuclear Data Library), it reaches values exceeding 900 barn for thermal neutrons, while cross-sections of (^{7}Li,n) are much lower, as shown in Chapter 12 of Ref. [2]. Therefore, lithium heavily enriched (> 80%) with ^{6}Li is a constituent of all candidate materials considered for the absorber. Several ceramics have been tested: Li_2ZrO_3, Li_8ZrO_6, Li_2TiO_3, $LiAlO_2$, Li_2SiO_3 and Li_4SiO_4. The other candidates are lithium oxide (Li_20), mixture of lithium and beryllium fluorides $(LiF)_2$–BeF_2 called Flibe (Li_2BeF_4) and Li17–Pb eutectic in the form of a liquid alloy or pebbles.

In the (^{6}Li, n) process one neutron produces only one tritium atom. To increase the efficiency of tritium breeding a neutron multiplier is to be added. It is mainly beryllium, but also lead (Pb) is considered in some concepts of tritium breeding blankets:

$$^{9}\mathrm{Be} + \mathrm{n} \rightarrow 2\alpha + 2\mathrm{n}' - 2.5\,\mathrm{MeV} \quad (E_{th} = 2.7\,\mathrm{MeV}), \tag{11}$$

$$^{208}\mathrm{Pb} + \mathrm{n} \rightarrow {}^{207}\mathrm{Pb} + 2\mathrm{n}' - 7.4\,\mathrm{MeV}. \tag{12}$$

There are also side reactions with low cross-sections leading to the production of tritium and helium and, eventually, to the accumulation of tritium in He bubbles formed in Be:

$$^{9}\mathrm{Be} + \mathrm{n} \rightarrow \alpha + {}^{6}\mathrm{He} \quad (E_{th} = 0.67\,\mathrm{MeV}) \tag{13}$$

$$^{6}\mathrm{He}\ (\beta^{-}) \rightarrow {}^{6}\mathrm{Li} \quad (E_{\beta} = 3.508\,\mathrm{MeV}, \quad t_{1/2} = 0.807\,\mathrm{s}) \tag{14}$$

$$^{9}\mathrm{Be} + \mathrm{n} \rightarrow {}^{7}\mathrm{Li} + \mathrm{T} - 10.40\,\mathrm{MeV} \quad (E_{th} = 11.6\,\mathrm{MeV}). \tag{15}$$

Several concepts for tritium breeding modules (TBM) are considered to be constructed by different ITER partners. The modules are to be consecutively tested on three ports (as currently proposed) once the reactor is ready to start full D–T operation. The list comprises water-cooled ceramic breeder (WCCB) [12], and series of helium-cooled modules: lithium–lead (HCLL) [13, 14], pebble bed (HCPB) [15], dual coolant lithium–lead (DCLL) [16] and ceramic breeders such as He-cooled (HCCB) [17] and lithium–lead ceramic (LLCB) [18, 19]. Some of those concepts [13, 14] are also being developed for a demonstration reactor of fusion power plant: DEMO. This huge effort focused on the development of blanket modules clearly shows that the success of fusion will depend on the breeding ratio which must be greater than one to supply enough fuel for the self-sustaining operation [20]. In calculations one takes into account expected breeding efficiency, the amount spent in burning plasma and tritium losses through natural radioactive decay, permeation through structures and long-term retention in PFC: the latter is discussed in "Plasma–Wall Interactions and Plasma-Facing Materials" section. The efficiency is strongly influenced by geometrical structure, breeder materials, neutron multipliers in the blanket system. The minimum requirement is the breeding ratio of 1.1. The estimates by Sawan and Abdou [21] have led to the value of 1.2. It must be stressed that the latter value is only a results of calculations which cannot be verified in any other system than the fusion reactor itself, as it requires the full fuel cycle to be in place. A simplified tritium cycle is shown in Fig. 1: neutrons originating from the D–T reaction interact in the blanket with lithium generating tritium which must be extracted to fuel the fusion process.

Availability of other reactants needed for fusion and tritium breeding, deuterium and lithium, does not present major difficulties. These are easily achievable reactants because they are found in nature in inexhaustible supply. Non-radioactive deuterium (natural abundance 0.015%) is extracted from sea water ($\sim$ 33.3 g D/m^3). Also lithium can be extracted from sea water (main assumed source containing 0.1–0.2 ppm of ^{7}Li + ^{6}Li) or obtained from common minerals such as lepidolite K (Li, Al)$_3$(Al, Si, Rb)$_4$ O_{10}(F, OH)$_2$, spodumene $LiAl(SiO_3)_2$, petalite $LiAlSi_4O_{10}$, amblygonite (Li, Na)$AlPO_4$(F, OH) and others.

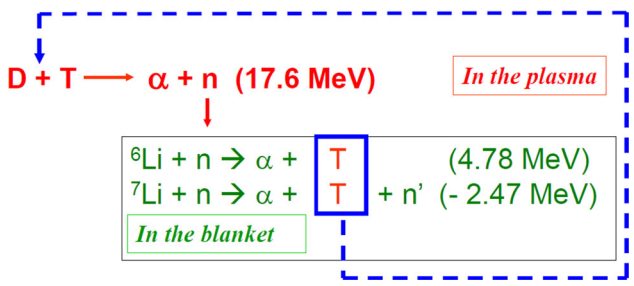

Fig. 1 Basic scheme of tritium cycle: neutrons originating from the D–T reaction interact in the blanket with lithium generating tritium which must be extracted to fuel the fusion process

Tritium Plant

All tritium from the reactor systems, both from the breeding blanket, exhausted from the torus (i.e. not used fuel pumped out from the reactor because only a small fraction of D–T mixture will be burnt in fusion reactions) and extracted from the cooling media (water and He), must be collected and handled by installations of the Tritium Plant before it can be used for plasma fuelling. Collected tritium must first undergo separation and purification from other gases used in a tokamak operation or also from various impurities in the vacuum system. Quantitative isotope separation is the next step.

Through the gas distribution system one supplies to the torus not only fuel, D_2, $D_2 + T_2$, T_2, but also light gases for wall cleaning (^{4}He and H_2) or ^{3}He if needed for resonance heating and heavier species for plasma edge cooling (i.e. impurity seeding) or massive gas injection, i.e. for disruption mitigation: N_2, Ne, Ar and possibly Kr. As a result, not spent fuel, other injected gases and volatile impurities are in the exhaust pumped out from the torus. Tritiated species occur in the form of gas molecules (I_2, where I denotes a mixture of hydrogen isotopes), water (I_2O), hydrocarbons (C_xI_y), carbon oxides (mainly monoxide CO), possibly ammonia (NI_3 if nitrogen is used for plasma edge cooling) and also mixtures containing I–O–C–N or other impurities forming volatile products. Carbon-containing compounds are mentioned here, because some carbon impurities will always be present even in a machine with all PFC made of metals, because of intrinsic impurities of in-vessel materials, a result of leaks and also contamination of components during the installation phase.

Separation methods comprise cryogenic distillation, condensation, electrolysis, diffusion via palladium (Pd) membranes, catalytic processes: oxidation of C_xI_y to CO or CO_2 and I_2O, decomposition of I_2O, C_xI_y, NI_3 and vapour stage exchange:

$$CO + I_2O \leftrightarrow CO_2 + I_2 \quad \text{[water gas shift]} \tag{16}$$

$$CI_4 + I_2O \leftrightarrow CO + 3I_2 \quad \text{[steam reforming]} \tag{17}$$

$$CI_4 \leftrightarrow C + 2I_2 \quad \text{[methane cracking]} \tag{18}$$

$$NI_3 \leftrightarrow N_2 + 3I_2 \quad \text{[ammonia cracking, Co-, Ni-based catalysts]} \tag{19}$$

$$2I_2O \leftrightarrow O_2 + 2I_2 \quad \text{[photocalysis, electrolysis]}. \tag{20}$$

Catalytic cracking or decomposition of ammonia is the reverse reaction of the Haber–Bosch synthesis of ammonia.

Isotope Separation Station (ISS) with cryogenic installations is in the heart of the Tritium Plant. Differences in the boiling point of hydrogen isotopes, helium and remaining impurity gases allow for final purification and separation of species. Boiling points (T_B) of hydrogen isotopes are: 20.28 K (H_2); 22.13 K (HD), 23.67 (D_2) and 25.04 K (T_2). At these temperatures, helium isotopes (^{3}He and ^{4}He) are in the gaseous form, while other species, including neon (T_B = 27.104 K and melting at 24.56 K) had already been removed. A schematic flow diagram in an isotope separation facility based on the Tritium Separation Test Assembly (TSTA) operated until 1997 in Los Alamos National Laboratory, can be found in [22], while the information regarding the ITER fuel cycle have been presented by Mardoch [23]; it is also described in [2]. All tritium for introduction to the torus (freshly supplied to the reactor site and that leaving the ISS) must be stored in uranium or Co-Zr beds at low temperature. This is to ensure precise dosing and to avoid uncontrolled release of the radioactive gas. Also deuterium for the gas introduction system is stored in U-beds. The discharge of pure gases from the beds is realised at elevated temperature of about 720 K [7].

System for processing exhaust gases from the torus requires pumps fully compatible with tritium to ensure safe handling and closed gas loop for T_2 and D_2. They must be available from the very start of the D–D operation. The throughput is at the level 200 Pa m^3s^{-1} with 10% impurities. Testing of a prototype is ongoing also under tritium conditions [24].

Plasma–Wall Interactions and Plasma-Facing Materials

In a controlled thermonuclear device with magnetic confinement plasma–wall interactions (PWI) comprise all processes involved in the energy and mass exchange between the plasma and the surrounding wall. A scheme showing main processes of PWI is shown in Fig. 2, while a very comprehensive description of interactions and their consequences can be found in [25–27]. Energy leaves plasma in the form of electromagnetic radiation and kinetic energy of particles. Plasma-surrounding wall is irradiated by ions, charge-exchange neutrals, electrons, neutrons and photons originating from nuclear (γ) and electronic processes (X, UV). All of them modify material properties, from the very surface to the bulk. Simultaneously plasma is modified by impurities released by erosion processes from the wall.

Bombardment by particles originates from the fact that the discharge time is much longer than the particle confinement time ($t_{discharge} \gg \tau_p$). Some incoming particles are reflected and they instantly return to plasma, some remain in the wall for certain time before being released (this is recycling), but a fraction is trapped. The latter is referred to as long-term retention. Particle impact causes

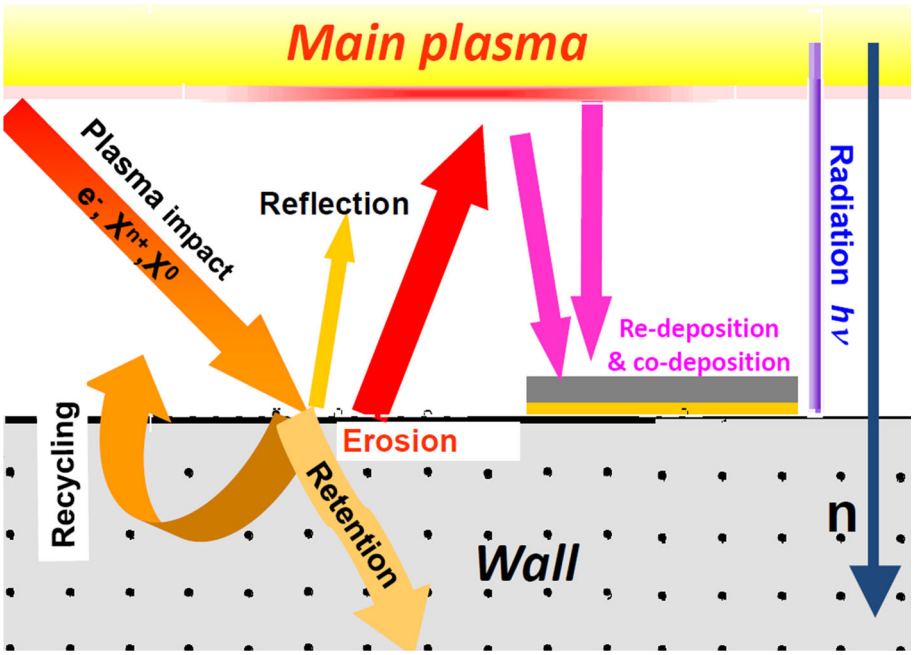

Fig. 2 Main processes in plasma–wall interactions

wall erosion. Species removed from the wall are ionised when they enter plasma and then they transported along magnetic field lines. Eventually, material removed from the wall, unless it is pumped out, must be deposited in another location either close or distant from the place of origin. In this process various plasma impurities are re-deposited together with fuel atoms thus forming mixed-material co-deposited layers. There is a complex chain of material migration: (a) erosion, (b) transport, (c) deposition being actually a co-deposition of fuel and impurity atoms, (d) re-erosion, (e) transport (f) re-deposition, etc. [27]. Micrographs in Fig. 3 show the appearance of such beryllium-rich (Fig. 3a) layers and the melt damage to a tungsten plate tested in a tokamak (Fig. 3b). Stratified Be-rich co-deposits are structurally very similar to carbon-rich layers observed in tokamaks with graphite walls. It is stressed here that this type of surface modification is not connected with neutrons, but the formation of mixed-material deposits will have an impact on the distribution of radioactivity (accumulation of T and also n-activated species) in a reactor. Also the change of tungsten PFC structure after melt events may eventually have an impact on mechanical properties of material under neutron irradiation.

The main erosion mechanisms are: physical sputtering, chemical erosion, melting and melt layer splashing, evaporation, arcing, photo- and electron-induced desorption. Neutron irradiation changes properties not only of plasma-facing, but also of structural, functional (e.g. T breeders and diagnostics) and other materials being in the neutron field. In summary, PWI processes are necessary, unavoidable and destructive. All these three aspects are to be considered in a list of requirements for different categories of fusion reactor materials.

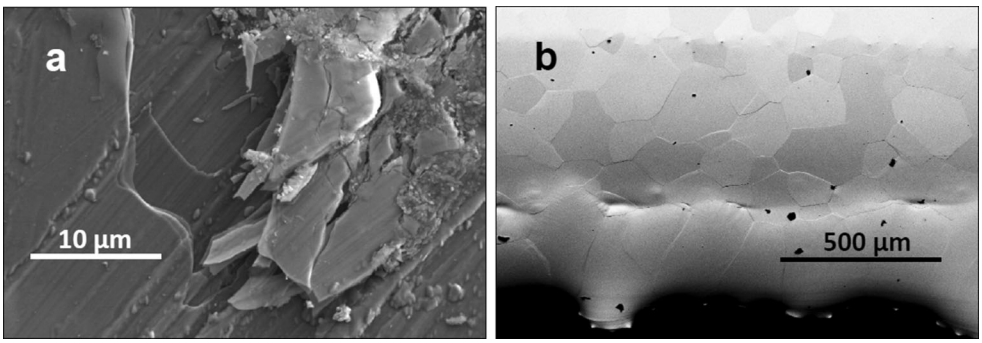

Fig. 3 Surface topography of materials exposed to plasma in tokamaks: **a** beryllium-rich co-deposit and **b** melt damage to a tungsten plate. Authors: Dr. E. Fortuna-Zalesna (Fig. 3a) and Dr. E. Wessel (Fig. 3b)

In-Vessel Materials and Components

Whichever product is manufactured, whether small or huge, it must possess some indispensable features to find a customer: functionality, stability, durability, reliability. The product must also comply with safety requirements and standards. These features are related to a broad range of factors including thorough design and selection of materials. A fusion reactor makes the requirements even more stringent. It is a nuclear device which must produce energy and—at the same time—must comply with safety requirements regarding the construction, operation, maintenance and decommissioning phases. It must also satisfy licensing criteria set by atomic agency authorities. The temperature gradients between the plasma and the surrounding wall are probably the greatest in the Universe and the operation is associated with intense nuclear radiation. Therefore, the technology for next-step devices with the D–T fuel presents challenges not encountered in present-day machines. This includes development and construction of components capable of reliable performance under exposure to intense particle fluxes and resulting high heat loads (above 10 MW m^{-2}) in highly radioactive environment. All starts with materials whose properties must satisfy several criteria. Compatibility with high vacuum for all in-vessel materials and high thermal conductivity of plasma-facing materials and components are the prerequisites. Others requirements for PFM comprise resilience to thermal shocks, high melting point, low-Z to reduce energy radiation losses by plasma contaminants, low neutron activation, low affinity towards chemical erosion resulting in the formation of volatile products, low sorption of hydrogen isotopes and high affinity to plasma impurity species (e.g. oxygen) towards the formation of stable non-volatile compounds. Another indispensable feature is the compatibility of PFM with the heat sink structure (mainly Cu alloyed with admixtures of chromium and zirconium) to ensure efficient and reliable active cooling. All these criteria together cannot be fully met by any single element, compound, alloy or composite material. Underlying physics and chemistry of erosion processes cannot be changed or eliminated, hence the goal of plasma edge engineering is to improve the control of interactions by optimizing the reactor operation scenarios and by the selection of the best-possible materials.

For over 2 decades, carbon, beryllium and tungsten were the major candidates for PFC. Advantages and drawbacks have been studied and discussed in detail [26–28]. Three materials were supposed to be used in ITER: beryllium on the main chamber wall, while tungsten and carbon in the form of fibre composites (CFC) in the divertor. The latter material was on the list because of not melting, high thermal conductivity (γ), excellent power handling capabilities and very low activation. However, high erosion rates by plasma and the formation of thick co-deposited layers (> 100 μm) rich with hydrogen isotopes (10–25 at.%) would lead to unacceptable levels of tritium inventory in the machine, especially in remote areas in the divertor. The full seriousness of the process and its detrimental impact on the reactor economy and safety was understood after the full D–T campaign in JET [7, 29–31]. As a result, a large-scale test in JET with a metal wall, beryllium and tungsten, was decided: JET with the ITER-Like Wall (JET-ILW) [32–34]. Distinctly reduced fuel inventory in the metal surrounding in comparison to the operation with carbon PFC in JET (JET-C) led to a major scientific and technological decision on resigning from using carbon in the ITER divertor [35]. This decision has also economical and safety aspects related to the motivated expectation of lowering the in-vessel inventory of tritium.

Radiation-Induced Effects

Neutrons pass the armour and structural materials of the blanket leading to the volumetric change of material composition by transmutation and to the damage of the crystalline lattice. This changes material properties and performance. A brief overview of major consequences for structural and diagnostic materials is presented in this section.

Transmutation

Transmutation is a conversion of one nucleus to another. It is the change in a nucleus structure, i.e. the formation of different isotope(s) or element(s) induced by bombarding the nucleus with particles or high-energy photons, (via Compton effect) which can induce nuclear reactions [36–41]. All isotopes undergo transmutation whose efficiency is related to the energy-dependent cross-section, $\sigma(E)$, of a given n-induced nuclear reaction.

Transmutation processes have serious consequences for all reactor materials, both structural and functional, and for reactor safety. This comprises the change of nuclear and also chemical composition of wall components which has a direct impact on thermomechanical properties: heat conductivity and capacity, and on linear expansion coefficient. It also induces radioactivity by transmuting stable nuclei to radioisotopes of different lifetime.

In the following, several examples will be considered for plasma-facing (Be, W and C) and structural materials (low-activation alloys). The transmutation of ^{9}Be (the only Be stable isotope) has already been partly addressed in reactions (11), (13) and (15). Another process is the

activation of ^{9}Be to radioactive ^{10}Be, $t_{1/2} = 1.387 \times 10^{6}$ year. It decays by β^{-} emission to stable ^{10}B.

Carbon has two stable isotopes: ^{12}C (abundance 98.93%) and ^{13}C (1.07%). The efficiency of transmutation to a radioactive isotope ^{14}C (β^{-}, 0.156 MeV, $t_{1/2}$ = 5730 year, specific activity 1.65×10^{11} Bq/g) in a fusion device would be very low because cross-sections for neutron capture by both stable isotopes are very low on the level of a few micro-barn ($1b = 1 \times 10^{-28}$ m^2).

Tungsten has four stable isotopes and one of a very long half lifetime: ^{180}W (natural abundance 0.12%, $t_{1/2} = 1.8 \times 10^{18}$ year), ^{182}W (26.50%), ^{183}W (14.31%), ^{184}W (30.64%), ^{186}W (28.43%). First stages of transmutation for the two heaviest and most abundant isotopes are:

$$^{184}\mathrm{W}(\mathrm{n},\gamma)^{185}\mathrm{W}(\beta^{-}) \rightarrow ^{185}\mathrm{Re}(\mathrm{n},\gamma)^{186}\mathrm{Re}(\beta^{-}) \rightarrow ^{186}\mathrm{Os} \quad (21)$$

$$^{186}\mathrm{W}(\mathrm{n},\gamma)^{187}\mathrm{W}(\beta^{-}) \rightarrow ^{187}\mathrm{Re}(\mathrm{n},\gamma)^{188}\mathrm{Re}(\beta^{-}) \rightarrow ^{188}\mathrm{Os} \quad (22a)$$

$$^{186}\mathrm{W}(\mathrm{n},\gamma)^{187}\mathrm{W}(\beta^{-}) \rightarrow ^{187}\mathrm{Re}(\mathrm{n},2\mathrm{n})^{186}\mathrm{Re}(\beta^{-}) \rightarrow ^{186}\mathrm{Os}. \quad (22b)$$

In all cases the transmutation leads to the formation of ^{186}Os (stable isotope) which is then transmuted to other nuclei. Though the same intermediate isotope is produced in Reactions (21, 22a, 22b) the rates of processes are distinctly different because of differences in cross-section of respective steps. Temporal evolution of the composition change for tungsten and W alloys under ITER and fusion power plant conditions has been calculated by Gilbert and Sublet [37]. Besides the main products, i.e. Re and Os, there are some quantities of tantalum, hafnium, hydrogen, helium and, in the case of a power plant reactor also platinum and iridium. It is predicted that in ITER after 14 years of operation there will be 0.2 (at.%) of Re in W, while after 5 years of reactor operation Re and Os will constitute around 10 (at.%) of the composition. The new alloy will also contain H, He and a large number of other species, such as Ta, Hg, Pt. Calculations for transmutation of other elements are in [38–41]. One expects that the change of chemical composition would not be uniform through the bulk because cross-sections change with the neutron energy loss by stopping in the lattice. It should also be stressed that activation is to be taken into account in the case of plasma edge cooling, especially when the use of heavy gases, e.g. Kr, is considered [41].

Basic physics underlying the transmutation leading to the formation of radioactive nuclei cannot be overcome. The only way to minimize its effects is to use low-activation materials, i.e. materials containing elements of low cross-sections for transmutation or elements whose transmutation products are either non-radioactive or short-lived isotopes. It is clear that products and related radioactivity (i.e. energy spectrum and lifetime) strongly depend on the initial composition of the irradiated material. It also implies that not only major constituents should undergo low activation but also the quantity and quality of admixtures and impurities must be strictly controlled. For instance, while major constituents of low-activation vanadium alloys (V–3Ti–1Si) transmute to isotopes of short lifetime (^{46}Sc, ^{47}Sc, ^{51}Cr), the presence of even trace quantities of nickel impurities transmuted to ^{60}Co leads to a highly activated product ($t_{1/2}^{60}Co$ = 5.27 year). The same remark regarding Ni may be applied to EUROFER-97, low-activation high-chromium alloy, developed for fusion reactor technology [42]. Fabrication of components containing low activation and high purity constituents is of great importance but also a reasonable approach is to be place taking into account limits in purification processes and their impact on the cost of production.

An important consequence of nuclear reactions is simultaneous formation of other transmutation products. In general, they belong to three categories:

1. Gaseous species such as hydrogen isotopes and helium: (n, p), (n, np), (n, d), (n, t) (n, α), (n, nα), (n, ^{3}He)
2. Gamma radiation: (n, γ), (n, n′γ)
3. Neutron breeding: (n, 2n), (n, 3n).

Particular attention should be given to processes of the first-group which generate hydrogen isotopes (H, D, T) or helium (^{3}He, ^{4}He). Gases are accumulated in the crystal lattice and they form bubbles and blisters. Bubbles are formed not only in the surface layer but also in the bulk. In a critical situation when the pressure of the accumulated gas overcomes a certain limit, blisters explode leading to the exfoliation; an example is shown in Fig. 4.

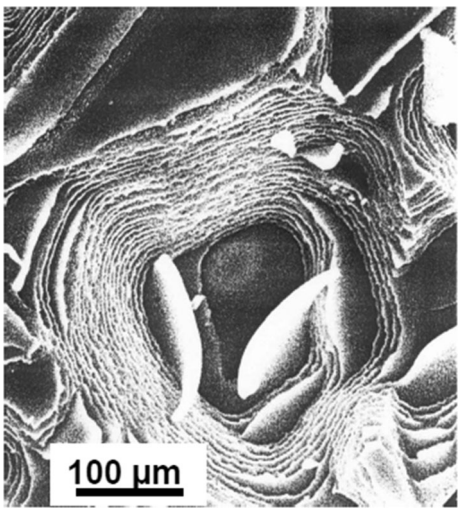

Fig. 4 Exfoliation of steel caused by high-dose irradiation

Radiation Damage

Energetic particles transfer their energy to the irradiated target through inelastic (electronic) and elastic (nuclear) interactions. Fundamental processes have been reviewed in [43, 44]. Inelastic energy losses lead to the ionisation and have a serious impact on electrical properties, while elastic stopping mean interactions with the lattice and—as a consequence—modification of the crystalline structure.

The measure of damage to a crystalline matter caused by bombardment with energetic particles is expressed in terms of so-called *displacement per atom* (dpa), i.e. the number of times each atom is dislodged from its place in the crystal by radiation. In other words, 1 dpa is equivalent to displacing all atoms once from their lattice sites. The cross-section for processes of neutron displacement damage is generally in the range from 1 to 10 barns. Damage depends on the fluence (total dose) and, in some cases, also on the neutron flux, though the latter is, however, is questionable. The dependence has been reported in earlier works [45, 46] but recent studies have not provided conclusive confirmation [47–49]. In carbon, beryllium and ceramic materials 1 dpa is produced by a neutron dose of around 1×10^{25} m^{-2}. Volumetric damage leads to the formation of dislocations, interstitials, voids and vacancies, in the crystal lattice. This results from the direct knock-on of atoms and/or ions from their sites. Knock-on atoms of sufficiently high energy initiate further displacements by producing collision cascades. Dislocation is defined as a line, plane or region in which there is a discontinuity in the regularity of the lattice. Voids and vacancies are the empty spaces formed by shifting atoms from their original sites. The distortion of crystals is further enhanced by the formation of gaseous products. As a consequence, all material properties are affected and deteriorated: chemical and physical such as thermo-mechanical, electrical conductivity. Phonon scattering on lattice defects has implications for thermal conductivity [50] leading to the decrease of that crucial parameter for materials of plasma-facing components and tritium breeding modules. The presence of voids and the related formation of gas bubbles leads to swelling. In the end effect the volume of metals [51–55] or ceramics is increased. On the contrary, carbon fibre composites (no bubble formation) shrink [56]. This in turn, leads to the significant drop in thermal conductivity, even by 70% from the original value [56]. 1 dpa typically results in 1% volume change. Swelling of a metal crystal changes drastically its mechanical properties causing hardening and resultant increased brittleness (embrittlement). Ductility is decreased by the agglomeration of He and H bubbles at grain boundaries and densification of dislocation network. The extent of damage is reduced at elevated temperatures due to annealing. However, for obvious reasons the temperature of materials and components cannot be increased indefinitely. Therefore, efforts in irradiation tests are focused on the definition of material operation limits (lifetime) at various neutron dose and irradiation temperature.

Impact on Materials of Diagnostic Systems

Diagnostic tools are essential for the safe and efficient functioning of a reactor: for the machine protection, guiding operation scenarios and to support advanced plasma research. The required and essential features of diagnostics are: reliability, repeatability, resistance to radiation, resistance to heat and—last but not least—maintainability. Thousands of components of diagnostic systems belong to several categories: mechanical supports, feedthroughs, seals, bolometer substrates, pressure gauges, windows, mirrors, neutron detectors, optical cables, connectors including mineral-insulated (MI) cables. Most of them, besides, certain mirrors (so-called *first mirrors* as plasma-facing components of optical diagnostic systems) will be protected from the direct plasma impact, but they still will be in the neutron field of diverse intensity. A list of materials used in diagnostics comprises hundreds of different substances. Many of them are insulators: quartz, silica, aluminium oxide (sapphire), aluminium nitride, beryllium oxide, boron nitride, alumino-silicates, diamond and many materials doped with boron. MI cables are indispensable for reliable operation and signal transmission from magnetic coils and thermocouples. There is a very broad program for development of radiation-hard materials for the use in fusion [57, 58] and many other disciplines where strong particle and electromagnetic radiation is generated [59]. Under extreme environment insulating properties of ceramics are changed and mostly deteriorated. The presence of voids and bubbles increases diffusion which is particularly dangerous in the case of radioactive tritium. The content of Table 1 summarizes several most pronounced processes and consequences of the irradiation. Surface effects listed in the last row originate from plasma–material interactions which are responsible for erosion and deposition. They are of particular importance in the case of first mirrors, therefore, a comprehensive test is carried out for ITER [60–67] and DEMO [68–70] both in tokamaks and under laboratory conditions.

Material Testing

Material testing under as realistic as possible conditions is a crucial procedure in the qualification process of materials and components in every technology. Mechanical integrity

Table 1 Radiation-induced effects in diagnostic materials

Process	Consequences
Radiation-induced (enhanced) conductivity (RIC)	Excitation of electrons into a conduction band
Radiation-enhanced absorption (RIA)	Light transmission loss
Radiation-induced electrical degradation (RIED)	Permanent enhancement of the volume conductivity caused by bulk radiation-induced defects
Radiation-enhanced diffusion (RED)	Increased tritium mobility in ceramic windows
Radiation-induced electro-motive force (RIEMF)	Induced voltage between centre and outer conductors of MI cables
Surface effects by sputtering, re-deposition, impurity segregation, (melting, evaporation, splashing)	Degraded specular reflectivity by erosion and deposition. Contamination of mirrors

and durability of items are absolutely essential. In the nuclear sector the lifetime of items is of particular importance for at least two reasons: safety of operation and complex procedures in maintenance and exchange of components. As pointed out in "In-Vessel Materials and Components" section, thermal conductivity of plasma-facing materials is one of the most important factors in selection of materials for PFC. There are numerous examples showing a pronounced decrease of that parameter not only after high-dose irradiation [56], but even after doses corresponding to 0.1–0.3 dpa [71]. This is turn will have a crucial impact on heat transfer from a PFC to a cooling structure.

In every branch of fusion science technology there are areas to be further developed and/or explored on the way to a power station. In the domain of materials, the list of main tasks also comprises:

(1) Advances in technology of high purity and radiation hard materials;
(2) Determination of fuel retention especially in plasm a-facing and structural materials of tritium breeding modules, to enable best-possible predictions of tritium inventory and its impact on a whole fuel cycle in a reactor.

It all calls for testing of selected materials and components under large doses of high energy neutrons to recognize the impact on electrical and thermo-mechanical properties. The crucial point is to produce a reactor-relevant level of damage (> 20 dpa per year) [72] including the modification of elemental composition. This can only be achieved by the irradiation with high fluxes or fast neutrons as they interact with the surface and the bulk of components. In other words, testing of radiation damage in reactor materials requires an efficient high-flux source of high-energy neutrons. There are advanced plans for the construction of the facility. The project will be presented in "Material Testing Under High-Energy Neutron Flux" section. Currently, irradiations are carried out in nuclear reactors. This has facilitated studies of the neutron impact on creep, ductility, thermal conductivity, retention of hydrogen isotopes [51–56, 71, 73]. The latter is examined also in ion-irradiated targets as they are easily available and distinctly cheaper than specimens from nuclear reactors.

Simulation of Neutron-Induced Effects by Ions: Impact on Test Mirrors

Damage can also be simulated by ion irradiation [74–77]. With energetic heavy ions very high damaged rates of tens of dpa are obtained, but the irradiation cannot lead to transmutation accompanied by generation of helium and hydrogen. Also the simulation of bulk effects is very limited as the implantation depth does not exceed a few micrometres. However, in one domain bulk effects do not play major role: testing of metallic mirrors which will be crucial components in all optical spectroscopy and imaging systems [78]. The test briefly described below was related to the simulation of neutron-induced effects that may degrade mirror performance in DEMO.

For the reflectivity of mirrors only the surface region is important: the optically active layer (OAL) calculated according to the the Beer–Lambert law. Light intensity penetrating a metal target falls exponentially with a decay constant known as absorption coefficient which depends on material and wavelength. In polycrystalline molybdenum, i.e. the material on which the test was performed, for the visible part of the spectrum it is in the range from 12 nm at the wavelength of 400 nm to approx. 22 nm at 800 nm; a detailed graph is shown in [68]. From the nuclear point of view, Mo is not an ideal material, as it has seven naturally occurring isotopes, three of which are measurably unstable with very long half-live times of more than 10^{14} years. Transmutation of Mo leads to long-lived radioactive isotopes of technetium (Tc), niobium (Nb), zirconium (Zr), molybdenum itself, hydrogen and helium from (n, p), (n, α) and (n, nα) reactions. It should be stated that all candidate

materials for mirrors would be affected by neutrons in a reactor, i.e. undergo transmutation and activation. Moreover, there is no clear suggestion or indication regarding materials for mirrors in DEMO.

To simulate neutron-induced effects including both transmutation of Mo and generation of gaseous products the irradiation was done with 30 keV $^{98}Mo^{+}$, $^{93}Zr^{+}$ or $^{90}Nb^{+}$, 2 keV He^{+} and with 4 keV H_2^{+} corresponding to 2 keV for a monoatomic beam. Irradiation with the major transmutation product (technetium) could not be performed, because all Tc isotopes are radioactive. It would enormously increase cost of the test and would simultaneously limit the range of post-irradiation analyses. The selection of respective ion energies was based on predictive modelling using SRIM [79] in order to match the thickness of OAL, i.e. to deposit ions within that surface layer. All experimental details can be found in [68, 69]. The $^{98}Mo^{+}$ ions were used to produce damage, while the irradiation with zirconium or niobium was done, because both elements are formed as transmutation products in neutron-irradiated Mo. The amount of Zr and Nb would be at the level of 1×10^{14} cm^{-2} and 1×10^{13} cm^{-2} in the surface layer of 15 nm. The damage to the surface layer (so-called *first wall damage*) of Mo in a DEMO reactor is estimated at the level of 7 dpa per year and this would be accompanied by the presence of 45 appm of He, 479 appm of H [37, 40]. In the irradiation higher doses of H and He were used because these species, as charge exchange neutrals from plasma, may and will also interact with first mirrors.

Plots in Fig. 5a show the total reflectivity changes, in comparison to the initial reflectivity, of a Mo mirror following the irradiation with $^{98}Mo^{+}$ ions to the dose of 15×10^{14} cm^{-2} corresponding to 10 dpa (Fig. 5b). The diffuse reflectivity of the initial mirrors was 0.5% and increased to 1% after the irradiation. Therefore, total reflectivity represent specular component which a figure of merit for mirrors. In the visible range the reflectivity increases with fluency. It is related to the removal of molybdenum oxides from the surface [63]. The reflectivity in the near infrared range decreases by up to 5% due to the damage caused by implantation. The same result was obtained when the irradiation was performed at 573 K. Significant changes are caused by the irradiation with 3×10^{17} He/cm^2 as shown in Fig. 5b. Reflectivity decreases by approximately 20% with some differences dependent on the wavelength. Additional decrease was induced by irradiation with a H^{+} beam [69]. These changes are caused by the gas accumulation in the bubbles beneath the surface, up to the depth of 30–40 nm, thus modifying OAL. They are clearly visible on the cross-section shown in Fig. 6 for a He bombarded mirror.

It is perfectly well understood energy spectra of neutrons in the reactor (up to 14 MeV) and those of ions

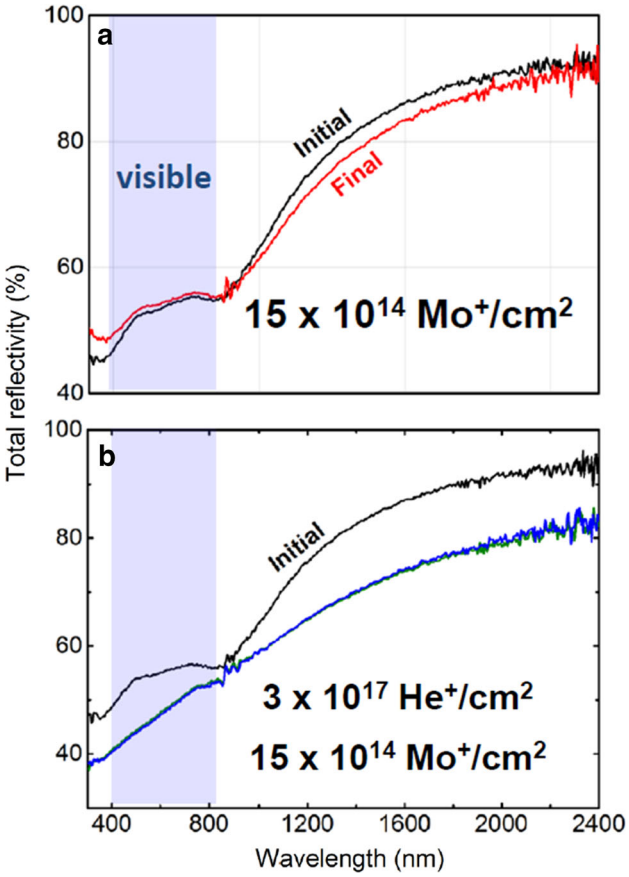

Fig. 5 The change of reflectivity in molybdenum test mirrors after irradiation with: **a** $^{98}Mo^{+}$ corresponding to 10 dpa; **b** both with He and $^{98}Mo^{+}$ beams

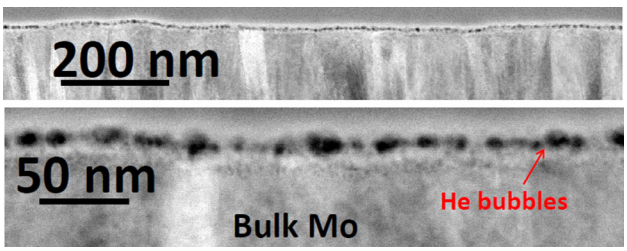

Fig. 6 STEM images of FIB-cut lamellae from the near-surface region of the Mo^{+} and He^{+} irradiated mirror. Author: Dr. Justyna Grzonka

(2–30 keV) are different. The modification and damage generated in mirrors under ion irradiation is not equal to that caused by neutrons, but the test under fully realistic conditions will become possible only in a real working fusion reactor, where all synergistic effects of material migration processes and neutron irradiation occur simultaneously. However, results of even such limited testing indicate that the major impact on the degradation of optical properties will be caused by H and He interaction, rather

charge exchange species than those formed by transmutation.

Material Testing Under High-Energy Neutron Flux

High-flux testing requires a construction of an efficient test facility capable of simulating the neutron energy spectrum of a D–T fusion reactor. Over the years, different concepts of neutron sources have been proposed. Taking into account the required neutron flux and energy spectrum to simulate the irradiation conditions of plasma-facing components in a reactor the most promising and relevant sources are those based on the ^{7}Li(d, 2n)^{7}Be, ^{6}Li(d, n)^{7}Be nuclear reactions (deuteron energy 30–40 MeV) generating neutrons with the energy spectrum peaking at around 14 MeV. Already in year 1976 a concept based on the deuteron irradiation of a lithium target was proposed [80]. In 1992 this approach using high-current deuterium beams was selected in year 1992 for the International Fusion Materials Irradiation Facility (IFMIF) [81] and in following years a conceptual design and technical specifications based scientific and engineering analyses were detailed and presented in year 2004 as a joint effort of EU, Japan, Russian Federation and the USA. In June 2007 the IFMIF-EVEDA project was established by the EU and Japan. EVEDA stands for Engineering Validation and Engineering Design Activities. There are three major components to be constructed, assembled and operated together to validate main technological challenges:

1. Accelerator facility,
2. Target facility (lithium loop),
3. Test facility (material irradiation chamber).

The project is based at the International Fusion Energy Research Centre (IFERC) in Rokkasho, Japan. Prototypes of three crucial facilities are either in operation or being manufactured. Respective modules of the accelerator, Linear IFMIF Prototype Accelerator (LIPAc), are manufactured mainly in EU (Belgium, France, Italy, Spain, some parts in Japan) and then shipped to IFERC, where the assembly takes place. The LIPAc is to prove the operation required for the first superconductive accelerating stage of IFMIF: 9 MeV, 125 mA of continuous wave D^{+} current resulting in a power of 1.125 MW that will validate the mastering of the space charge issues which are more relevant at low energies. Figure 7 shows the scheme of the LIPAc. All details about the program can be found in [82, 83].

The lithium target, EVEDA Lithium Test Loop (ELTL), was designed, assembled and operated at the Oarai Research and Development Center, Japan. Details about lithium technology for IFMIF are in [84], while the Li loop is described in [85, 86]. The aim was to prove the feasibility of technology, in particular to validate hydraulic stability of the Li target at a velocity up to 20 m s^{-1} under a vacuum condition of 10^{-3} Pa. A total of 2.5-t Li was placed in the ELTL chamber under clean controlled conditions to avoid any contamination by oxygen, nitrogen and water vapour. The 20 m high facility matched conditions required for the lithium loop exploitation at IFMIF: flow rate of 20 m s^{-1} at 300 °C, while IFMIF requires 15 ms^{-1} at 250 °C. The amplitude of the free surface stability is within +/1 mm at nominal flow conditions. The target of the ELTL is 100 mm wide, compared with the 260 mm of IFMIF, but with the same thickness of 25 ± 1 mm of the Li screen. Also the efficiency of liquid lithium purification from C, O, N and H has been successfully proven. In addition corrosion/erosion phenomena in steel conduits were studied and determined in the in LIFUS6 facility, a smaller Li loop operated at Brasimone, Italy [87].

High Flux Test Module (HFTM) is under fabrication at the Karlsruhe Institute of Technology (KIT), Germany. This is to house irradiated specimens at elevated temperatures in the range from 250 up to 550 °C with a maximum temperature spread of ± 3% within specimens inside a single capsule; 12 capsules are to be used. The cooling system is based on a fast flow of helium gas; it has been successfully validated in the HELOKA loop [88]. A test module to be placed in the medium flux region to assess the creep-fatigue behaviour under intense neutron and gamma irradiation was constructed and successfully validated at the Paul Scherrer Institute (PSI), Villigen, Switzerland.

In addition, remote handling studies for suitable replacement of the beam target have been carried out in Japan and Europe, together with the development in Japan of small specimens for fatigue, fracture toughness and crack growth. A set of small specimens for additional mechanical properties like tensile stress or creep has already been manufactured.

Successful operation of prototypes would mitigate risks for IFMIF which operation is planned to be based on 30–40 MeV from two continuous-wave linear accelerators with a total beam current of 2 × 125 mA. The neutron generation rate of some 10^{17} s^{-1} would result in a flux of some 10^{19} m^{-2} s^{-1} at the rear side of the target. Therefore, displacement damage (20 dpa per full power year) and transmutation products (He, H) in the irradiated material would match the neutron-induced effects anticipated in the fusion reactor environment. A drawing in Fig. 8 shows a scheme of the IFMIF assembly (length over 200 m) composed of the accelerator hall, lithium loop, test cell and a hall housing for facilities for post-irradiation examinations and for detritiation. The test cell will comprise a series of target chambers. The plan is install three chambers to allow

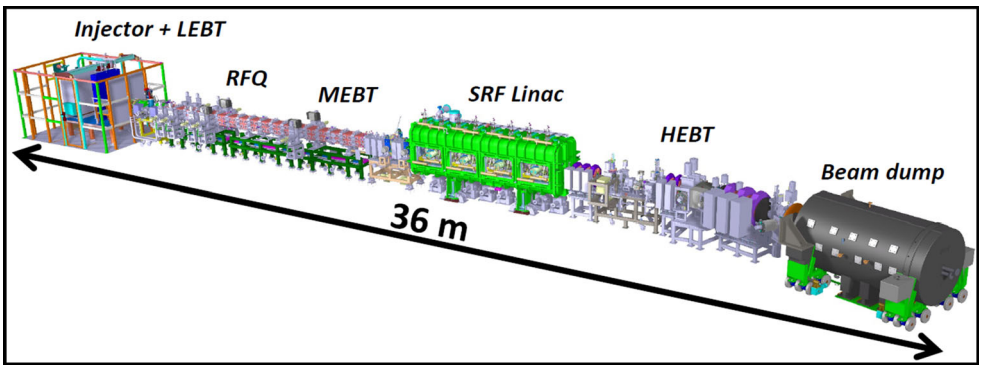

Fig. 7 A schematic drawing of LIPAc presently under installation and commissioning at IFERC. LEBT, low energy beam transport; RFQ, radio frequency quadrupole; MEBT, medium energy beam transport; SRF Linac, superconducting radio frequency linear accelerator; HEBT, high energy beam transport. *Source*: http://www.ifmif.org/?page_id=66

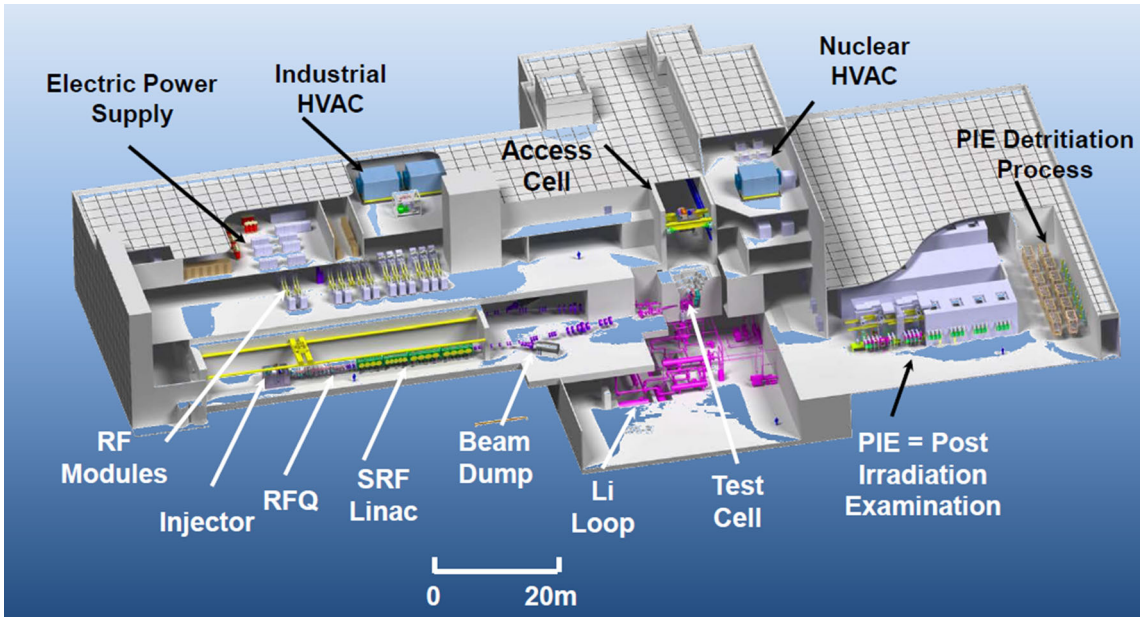

Fig. 8 A schematic plan of IFMIF. RFQ, Radio frequency quadrupole; SRF Linac, superconducting radio frequency linear accelerator; HVAC, Heating–Ventilation–Air Conditioning. Copyright ©Fusion for Energy (F4E)

for high flux irradiations in a volume of 0.5 L and lower dose irradiation in volumes of 6.0 and 7.5 L [70].

Concluding Remarks

Development and intense testing of materials and components belong to family of crucial elements for the progress in fusion science and technology. Having in mind scientific and technical challenges associated with the project, all efforts are to be made to ensure the best possible material selection, component manufacture and plasma edge engineering for a reactor-class machine. A reactor operated with the deuterium–tritium mixture is a nuclear device and—in addition to all machine construction and operation features—also radioactive aspects of fusion will undergo intense scrutiny. Proper testing and validation of material and component performance is essential to ensure their durability and integrity under high power loads in normal operation and in the case of off-normal events. Based on the best of our present knowledge we have to use and to develop tools, methods and materials best fitted for a steady–steady reactor operation. The entire dream and all hopes for commercial exploitation of controlled thermonuclear fusion for energy production depend on all aspects of power handling by PFC, efficient extraction of neutron energy and on efficient production, extraction and handling of tritium to fuel the reactor. In summary, it will depend on neutrons.

Acknowledgements This work has been carried out within the framework of the EUROfusion Consortium and has received funding from the Euratom research and training programme 2014–2018 under grant agreement No 633053. The views and opinions expressed herein do not necessarily reflect those of the European Commission.

References

1. H.-S. Bosch, G.M. Halle, Improved formulas for fusion cross-sections and thermal reactivities. Nucl. Fusion **32**, 611 (1992). https://doi.org/10.1088/0029-5515/32/4/I07/pdf
2. T. Tanabe (ed.), *Tritium: Fuel of fusion reactors* (Springer, Berlin, 2016)
3. J. Wesson, *Tokamaks*, 3rd edn. (Oxford Science Publications, Clarendon Press, Oxford, 2004)
4. E. Moses, Advances in inertial confinement fusion at the National Ignition Facility (NIF). Fusion Eng. Des. **85**, 983 (2010). https://doi.org/10.1016/j.fusengdes.2009.11.006
5. I. Hoffman, Review of accelerator driven heavy ion nuclear fusion. Matter Radiat. Extreme **3**, 1 (2018). https://doi.org/10.1016/j.mre.2017.12.001
6. P.-H. Rebut, Preliminary tritium experiment. Plasma Phys. Control. Fusion **34**, 1749 (1992). https://doi.org/10.1088/0741-3335/34/13/002
7. D. Stork et al., Systems for the safe operation of the JET tokamak with tritium. Fusion Eng. Des. **47**, 131 (1999). https://doi.org/10.1016/S0920-3796(99)00081-2
8. T.T.C. Jones et al., Technical and scientific aspects of the JET trace-tritium experimental campaign. Fusion Sci. Technol. **48**, 250 (2005). https://doi.org/10.13182/fst05-a922
9. C.H. Skinner, C.A. Gentile, J.C. Hosea, D. Mueller, J.P. Coad, G. Federici, R. Haange, Tritium experience in large tokamaks: application to ITER. Nucl. Fusion **39**, 271 (1999). https://doi.org/10.1088/0029-5515/39/2/410
10. J.N. Andrews, R.L.F. Kay, Natural production of tritium in permeable rocks. Nature **298**, 361 (1982). https://doi.org/10.1038/298361a0
11. M. Kovari, M. Coleman, I. Cristescu, R. Smith, Tritium resources available for fusion reactors. Nucl. Fusion **58**, 026010 (2018). https://doi.org/10.1088/1741-4326/aa9d25
12. M. Enoeda et al., R&D status of water cooled ceramic breeder blanket technology. Fusion Eng. Des. **89**, 1131 (2014). https://doi.org/10.1016/j.fusengdes.2014.01.035
13. G. Aiello et al., Development of the helium cooled lithium lead blanket for DEMO. Fusion Eng. Des. **89**, 1444 (2014). https://doi.org/10.1016/j.fusengdes.2013.12.036
14. J. Aubert et al., Status on DEMO helium cooled lithium lead breeding blanket thermo-mechanical analyses. Fusion Eng. Des. **109–111**, 991 (2016). https://doi.org/10.1016/j.fusengdes.2016.01.037
15. D. Carloni et al., Requirements for helium cooled pebble bed blanket and R&D activities. Fusion Eng. Des. **89**, 1341 (2014). https://doi.org/10.1016/j.fusengdes.2014.02.036
16. M.E. Sawan et al., Three-dimensional nuclear analysis for the US dual coolant lead lithium ITER test blanket module. Fusion Eng. Des. **85**, 1027 (2010). https://doi.org/10.1016/j.fusengdes.2010.01.002
17. K.M. Feng et al., New progress on design and R&D for solid breeder test blanket module in China. Fusion Eng. Des. **89**, 1119 (2014). https://doi.org/10.1016/j.fusengdes.2014.01.073
18. R. Battacharyay, Indian TBM team, Status of Indian LLCB TBM program and R&D activities. Fusion Eng. Des. **89**, 1107 (2014). https://doi.org/10.1016/j.fusengdes.2014.05.016
19. I.R. Kirillov et al., Results of lead–lithium ceramic breeder TBM conceptual design optimization. Fusion Eng. Des. **89**, 1421 (2014). https://doi.org/10.1016/j.fusengdes.2014.01.006
20. L.A. El-Guebaly, S. Malang, *Towards the Ultimate Goal of Tritium Self-Sufficiency*. http://fti.neep.wisc.edu/pdf/fdm1330.pdf
21. M.E. Sawan, M.A. Abdou, Physics and technology conditions for attaining tritium self-sufficiency for the DT fuel cycle. Fusion Eng. Des. **81**, 1131 (2006). https://doi.org/10.1016/j.fusengdes.2005.07.035
22. J.L. Anderson, P. LaMarche, Tritium activities in the United States. Fusion Technol. **28**, 479 (1995)
23. D.K. Murdoch et al., ITER fuel cycle development. Fusion Sci. Technol. **48**, 3 (2005)
24. Ch. Day, D.K. Murdoch, The ITER vacuum systems. J. Phys. Conf. Ser. **114**, 012013 (2008). https://doi.org/10.1088/1742-6596/114/1/012013
25. W.O. Hofer, J. Roth (eds.), *Physical processes of the interaction of fusion plasmas with solids* (Academic Press, New York, 1996)
26. G. Federici et al., Plasma-material interactions in current tokamaks and their implications for next step fusion reactors. Nucl. Fusion **41**, 1967 (2001). https://doi.org/10.1088/0029-5515/41/12/218
27. V. Philipps, P. Wienhold, A. Kirschner, M. Rubel, Erosion and redeposition of wall material in controlled fusion devices. Vacuum **67**, 399 (2002). https://doi.org/10.1016/S0042-207X(02)00238-5
28. J. Roth et al., Recent analysis of key plasma-wall interaction parameters for ITER. J. Nucl. Mater. **390–391**, 1 (2009). https://doi.org/10.1016/S0022-3115(00)00479-7
29. R.D. Penzhorn et al., Tritium depth profiles in graphite and carbon fibre composite material exposed to tokamak plasmas. J. Nucl. Mater. **288**, 170 (2001). https://doi.org/10.1016/S0022-3115(00)00705-4
30. J.P. Coad et al., Erosion/deposition issues in JET. J. Nucl. Mater. **290–293**, 224 (2001). https://doi.org/10.1016/S0022-3115(00)00479-7
31. M. Rubel et al., Beryllium and carbon films in JET following D–T operation. J. Nucl. Mater. **313–316**, 321 (2003). https://doi.org/10.1016/S0022-3115(02)01350-8
32. G.F. Matthews et al., ITER-like wall project overview. Phys. Scr. **T128**, 137 (2007). https://doi.org/10.1088/0031-8949/2007/T128/027
33. G.F. Matthews et al., JET ITER-like wall: overview of experimental program. Phys. Scr. **T145**, 014001 (2011). https://doi.org/10.1088/0031-8949/2007/T128/027
34. G.F. Matthews, Plasma operation with an all metal first-wall: comparison of an ITER-like wall with a carbon wall in JET. J. Nucl. Mater. **438**, S2 (2013). https://doi.org/10.1016/j.jnucmat.2013.01.282
35. S. Brezinsek, JET-EFDA Contributors, Plasma-surface interaction in the Be/W environment: conclusions drawn from the JET-ILW for ITER. J. Nucl. Mater. **463**, 11 (2015). https://doi.org/10.1016/j.jnucmat.2014.12.007
36. D. Li, K. Imasaki, K. Horikawa, S. Miyamoto, S. Amano, T. Mochizuki, Iodine transmutation through laser compton scattering gamma rays. J. Nucl. Sci. Technol. **46**, 831 (2012). https://doi.org/10.1080/18811248.2007.9711592
37. M.R. Gilbert, J-Ch. Sublet, Neutron-induced transmutation effects in W and W-alloys in a fusion environment. Nucl. Fusion **51**, 043005 (2011). https://doi.org/10.1088/0029-5515/51/4/043005

38. M. R. Gilbert, J.-C. Sublet, *Handbook of Activation, Transmutation, and Radiation Damage Properties of the Elements Simulated Using FISPACT-II & TENDL-2014; Magnetic Fusion Plants*. Technical report, CCFE-R(15)26, CCFE (2015)
39. M.R. Gilbert, J.-C. Sublet, *PKA Distributions of the Elements Simulated Using TENDL-2014*. Technical report CCFE-R(15)26-supplement, CCFE (2015)
40. M.R. Gilbert et al., An integrated model for materials in a fusion power plant: transmutation, gas production, and helium embrittlement under neutron irradiation. Nucl. Fusion **52**, 083019 (2012). https://doi.org/10.1088/0029-5515/52/8/083019
41. R.J. Walker, M.R. Gilbert et al., Neutron activation of impurity seeding gases within a DEMO environment. Fusion Eng. Des. **124**, 892 (2017). https://doi.org/10.1016/j.fusengdes.2017.01.057
42. J. Hoffmann et al., Improvement of reduced activation 9%Cr steels by ausforming. Nucl. Mater. Energy **6**, 12 (2016). https://doi.org/10.1016/j.nme.2015.12.001
43. N. Baluc, Materials for fusion power reactors. Plasma Phys. Control. Fusion **48**, B165 (2006). https://doi.org/10.1088/0741-3335/48/12B/S16
44. W. Yican, *Fusion Neutronics* (Springer, Berlin, 2017)
45. R.E. Larsen et al., Flux dependence of neutron enhanced diffusion in α-brass. Acta Metall. **12**, 1141 (1964). https://doi.org/10.1016/0001-6160(64)90093-8
46. S.R. MacEwen, The effect of neutron flux on dislocation climb. J. Nucl. Mater. **54**, 85 (1974). https://doi.org/10.1016/0022-3115(74)90079-8
47. D. Žontar et al., Time development and flux dependence of neutron-irradiation induced defects in silicon pad detectors. Nucl. Instrum Methods **A426**, 51 (1999). https://doi.org/10.1016/S0168-9002(98)01468-5
48. R. Stoller, The effect of neutron flux on radiation-induced embrittlement in reactor pressure vessel steels. J. ASTM Int. **1**, 1 (2004). https://doi.org/10.1520/JAI11355
49. F. Bergner et al., Flux dependence of cluster formation in neutron-irradiated weld material. J. Phys. Condens. Matter **20**, 104262 (2008). https://doi.org/10.1088/0953-8984/20/10/104262
50. M.V. Klein, Phonon scattering on lattice defects. Phys. Rev. **131**, 1500 (1963). https://doi.org/10.1103/PhysRev.131.1500
51. N. Sekimura, T. Okita, F.A. Garner, Influence of carbon addition on neutron-induced void swelling of Fe–15Cr–16Ni–025Ti model alloy. J. Nucl. Mater. **367–370**, 897 (2007). https://doi.org/10.1016/j.jnucmat.2007.03.065
52. I.A. Portnykh et al., The mechanism of stress influence on swelling of 20% cold-worked 16Cr15Ni2MoTiMnSi steel. J. Nucl. Mater. **367–370**, 925 (2007). https://doi.org/10.1016/j.jnucmat.2007.03.257
53. V.S. Neustroev, F.A. Garner, Severe embrittlement of neutron irradiated austenitic steels arising from high void swelling. J. Nucl. Mater. **386–388**, 157 (2009). https://doi.org/10.1016/j.jnucmat.2008.12.077
54. M. Rieth, A comprising steady-state creep model for the austenitic AISI L(N) steel. J. Nucl. Mater. **367–370**, 915 (2007). https://doi.org/10.1016/j.jnucmat.2007.03.062
55. S. Kondo, Y. Katoh, L.L. Snead, Cavity swelling and dislocation evolution in SiC at very high temperatures. J. Nucl. Mater. **386–388**, 222 (2009). https://doi.org/10.1016/j.jnucmat.2008.12.095
56. T.D. Burchell, Radiation damage in carbon–carbon composites: structure and property effects. Phys. Scr. **T64**, 17 (1996). https://doi.org/10.1088/0031-8949/1996/T64/002
57. G. Vayakis et al., Nuclear technology aspects of ITER vessel-mounted diagnostics. J. Nucl. Mater. **329–333**, 780 (2011). https://doi.org/10.1016/j.jnucmat.2011.01.081
58. M. Decreton, T. Shikama, E. Hodgson, Performance of functional materials and components in a fusion reactor: the issue of radiation effects in ceramics and glass materials for diagnostics. J. Nucl. Mater. **329–333**, 125 (2004). https://doi.org/10.1016/j.jnucmat.2004.04.012
59. A. Akindinov et al., Radiation hard ceramic RPC development. J. Phys. Conf. Ser. **798**, 012136 (2017). https://doi.org/10.1088/1742-6596/798/1/012136
60. M. Rubel et al., Mirror test for ITER at the JET tokamak: an overview of the programme. Rev. Sci. Instrum. **77**, 063501 (2006). http://link.aip.org/link/?RSINAK/77/063501/1
61. A. Litnovsky et al., Diagnostic mirrors for ITER: a material choice and the impact of erosion and deposition on their performance. J. Nucl. Mater. **363–365**, 1395 (2007). https://doi.org/10.1016/j.jnucmat.2007.01.281
62. M. Rubel et al., Overview of the second stage in the comprehensive mirrors test in JET. Phys. Scr. **T145**, 014070 (2011). https://doi.org/10.1088/0031-8949/2011/T145/014070
63. D. Ivanova et al., An overview of the comprehensive first mirrors test in JET with ITER-Like Wall. Phys. Scr. **T159**, 014011 (2014). https://doi.org/10.1088/0031-8949/2014/T159/014011
64. A. Garcia-Carrasco et al., Plasma impact on diagnostic mirrors in JET. Nucl. Mater. Energy **12**, 506–512 (2017). https://doi.org/10.1016/j.nme.2016.12.032
65. V. Voitsenya et al., Some problems of the material choice for the first mirrors of plasma diagnostics in a fusion reactor. Rev. Sci. Instrum. **70**, 790 (1999). https://doi.org/10.1063/1.1149402
66. M. Lipa et al., Analyses of metallic first mirror samples after long term plasma exposure in Tore Supra. Fusion Eng. Des. **81**, 221 (2006). https://doi.org/10.1016/j.fusengdes.2005.07.017
67. Y. Zhou et al., Study of first mirror exposure and protection in HL-2A tokamak. Fusion Eng. Des. **81**, 2823 (2006). https://doi.org/10.1016/j.fusengdes.2006.07.030
68. A. Garcia-Carrasco et al., Impact of helium implantation and ion-induced damage on reflectivity of molybdenum mirrors. Nucl. Instrum. Methods B **382**, 91–95 (2016). https://doi.org/10.1016/j.nimb.2016.02.065
69. M. Rubel et al., Metallic mirrors for plasma diagnosis in current and future reactors: tests for ITER and DEMO. Phys. Scr. **T170**, 014061 (2017). https://doi.org/10.1088/1402-4896/aa8e27
70. K. Ono et al., Effects of helium irradiation on degradation of optical properties of single and polycrystalline Mo mirrors for plasma diagnostics. Phys. Scr. **T138**, 014065 (2009). https://doi.org/10.1088/0031-8949/2009/T138/014065
71. J. Linke, Plasma facing materials and components for future fusion devices—development, characterization and performance under fusion specific loading conditions. Phys. Scr. **T123**, 45 (2006). https://doi.org/10.1088/0031-8949/2006/T123/006
72. J. Knaster, A. Möslang, T. Muroga, Materials reserach for fusion. Nat. Phys. **12**, 424 (2016). https://doi.org/10.1038/NPHYS3735
73. H. Fujita et al., Effect of neutron energy and fluence on deuterium retention behaviour in neutron irradiated tungsten. Phys. Scr. **T167**, 014068 (2016). https://doi.org/10.1088/0031-8949/T167/1/014068
74. O. Ogorodnikova et al., Annealing of radiation-induced damage in tungsten under and after irradiation with 20 MeV self-ions. J. Nucl. Mater. **451**, 379 (2014). https://doi.org/10.1016/j.jnucmat.2014.04.011
75. J. Grzonka et al., Electron microscopy observations of radiation damage in irradiated and annealed tungsten. Nucl. Instrum. Methods B **340**, 27 (2014). https://doi.org/10.1016/j.nimb.2014.07.043
76. S. Markelj et al., Deuterium retention in tungsten simultaneously damaged by high energy W ions and loaded by D atoms. Nucl. Mater. Energy **12**, 169 (2017). https://doi.org/10.1016/j.nme.2016.11.010
77. Z. Jiao, J. Michalicka, G.S. Was, Self-ion emulation of high dose neutron irradiated microstructure in stainless steels. J. Nucl.

Mater. **501**, 312 (2018). https://doi.org/10.1016/j.jnucmat.2018.01.054
78. A. Costley et al., Technological challenges of ITER diagnostics. Fusion Eng. Des. **74**, 109 (2005). https://doi.org/10.1016/j.fusengdes.2005.08.026
79. J.F. Ziegler et al., *The stopping and range of ions in solids*, 2nd edn. (Pergamon Press, New York, 1996)
80. P. Grand et al., An intense Li(d, n) neutron radiation test facility for controlled thermonuclear reactor materials testing. Nucl. Technol. **29**, 327 (1976)
81. A. Möslang et al., Suitability and feasibility of the International Fusion Materials Irradiation facility (IFMIF) for fusion materials studies. Nucl. Fusion **40**, 619 (2000). https://doi.org/10.1088/0029-5515/40/3Y/324
82. J. Knaster et al., Overview of IFMIF/EVEDA project. Nucl. Fusion **57**, 102016 (2017). https://doi.org/10.1088/1741-4326/aa6a6a
83. J. Knaster et al., IFMIF, the European–Japanese efforts under the Broader Approach agreement towards a Li(d, xn) neutron source: current status and future options. Nucl. Mater. Energy **9**, 46 (2016). https://doi.org/10.1016/j.nme.2016.04.012
84. J. Knaster, T. Kanemura, K. Kondo, An assessment of the evaporation and condensation phenomena of lithium during the operation of a Li(d, xn) fusion relevant neutron source. Heliyon **2**, e00199 (2016). https://doi.org/10.1016/j.heliyon.2016.e00199
85. H. Kondo et al., IFMIF/EVEDA lithium test loop: design and fabrication technology of target assembly as a key component. Nucl. Fusion **51**, 123008 (2011). https://doi.org/10.1088/0029-5515/51/12/123008
86. H. Kondo et al., Validation of liquid lithium target stability for an intense neutron source. Nucl. Fusion **57**, 066008 (2017). https://doi.org/10.1088/1741-4326/aa5fbd
87. J. Knaster, P. Favuzza, Assessment of corrosion phenomena in liquid lithium at T $<$ 873 K. A Li(d, n) neutron source as case study. Fusion Eng. Des. **118**, 135 (2017). https://doi.org/10.1016/j.fusengdes.2017.03.063
88. G. Schlindwein et al., Mechanical testing of the IFMIF HFTM-DC prototype during operation in the HELOKA-LP helium loop. Fusion Eng. Des. **124**, 1077 (2017). https://doi.org/10.1016/j.fusengdes.2017.03.138